

52542-59-3; $[\text{Mn}(\text{CO})_5]\text{Si}(\text{CH}_3)_3$, 26500-16-3; $[(\text{C}_5\text{H}_5)\text{Fe}(\text{CO})_2]\text{-Sn}(\text{C}_6\text{H}_5)_3$, 12132-09-1; $[(\text{C}_5\text{H}_5)\text{Fe}(\text{CO})_2]\text{COCHCHC}_6\text{H}_5$, 12216-33-0; $[(\text{C}_5\text{H}_5)\text{Fe}(\text{CO})_2]\text{COC}_6\text{H}_5$, 12154-94-8; $[(\text{C}_5\text{H}_5)\text{-Fe}(\text{CO})_2]\text{CH}_3$, 12080-06-7.

References and Notes

- (1) J. E. Ellis, *J. Organomet. Chem.*, **86**, 1 (1975).
- (2) R. B. King, *Acc. Chem. Res.*, **3**, 417 (1970).
- (3) R. E. Dessy, R. L. Pohl, and R. B. King, *J. Am. Chem. Soc.*, **88**, 5121 (1966).
- (4) R. B. King, "Organometallic Synthesis", Vol. 1, Academic Press, New York, 1965: (a) p 149; (b) p 152.
- (5) J. E. Ellis and E. A. Flom, *J. Organomet. Chem.*, **99**, 263 (1975).
- (6) D. L. Reger, D. J. Fauth, and M. D. Dukes, *Synth. React. Inorg. Met.-Org. Chem.*, **7**, 151 (1977).
- (7) R. B. King, *J. Inorg. Nucl. Chem.*, **25**, 1296 (1963).
- (8) J. E. Ellis and R. A. Faltynek, *J. Am. Chem. Soc.*, **99**, 1801 (1977).
- (9) J. E. Ellis, C. P. Parnell, and G. P. Hagen, *J. Am. Chem. Soc.*, **100**, 3605 (1978).
- (10) See, for example: "The Strem Catalog", Strem Chemicals, Inc., Newburyport, Mass.
- (11) J. P. Collman, *Acc. Chem. Res.*, **8**, 342 (1975).
- (12) See, for example: R. F. Heck, *Adv. Organomet. Chem.*, **4**, 243 (1966).
- (13) Sold under the following trade names by the Aldrich Chemical Co.: $\text{Li}(\text{C}_2\text{H}_5)_2\text{BH}$, Super-Hydride; $\text{Li}(\text{sec-C}_4\text{H}_9)_2\text{BH}$, L-Selectride; $\text{K}(\text{sec-C}_4\text{H}_9)_2\text{BH}$, K-Selectride.
- (14) Preliminary communication: J. A. Gladysz, G. M. Williams, W. Tam, and D. L. Johnson, *J. Organomet. Chem.*, **140**, C1 (1977).
- (15) J. A. Gladysz and W. Tam, *J. Am. Chem. Soc.*, **100**, 2545 (1978).
- (16) J. A. Gladysz and J. C. Selover, *Tetrahedron Lett.*, 319 (1978).
- (17) C. P. Casey and S. M. Neumann, *J. Am. Chem. Soc.*, **98**, 5395 (1976).
- (18) C. P. Casey and S. M. Neumann, *J. Am. Chem. Soc.*, **100**, 2544 (1978).
- (19) J. A. Gladysz and W. Tam, *J. Org. Chem.*, **43**, 2279 (1978).
- (20) M. Nitay and M. Rosenblum, *J. Organomet. Chem.*, **136**, C23 (1977).
- (21) D. W. McBride, E. Dudek, and F. G. A. Stone, *J. Am. Chem. Soc.*, **1752** (1964); R. E. Dessy, R. L. Pohl, and R. B. King, *J. Am. Chem. Soc.*, **88**, 5121 (1966).
- (22) D. F. Shriver, *Acc. Chem. Res.*, **3**, 231 (1970).
- (23) G. W. Parshall, *J. Am. Chem. Soc.*, **86**, 361 (1964).
- (24) R. E. Dessy, P. M. Weissman, and R. L. Pohl, *J. Am. Chem. Soc.*, **88**, 5117 (1966).
- (25) M. Rosenblum, *Acc. Chem. Res.*, **7**, 122 (1974).
- (26) Dr. C. F. Lane, Aldrich Chemical Co., personal communication.
- (27) C. A. Brown, *J. Am. Chem. Soc.*, **95**, 4100 (1973).
- (28) H. C. Brown, A. Khuri, and S. C. Kim, *Inorg. Chem.*, **16**, 2229 (1977).
- (29) H. C. Brown, S. Krishnamurthy, and J. L. Hubbard, *J. Am. Chem. Soc.*, **100**, 3343 (1978).
- (30) H. C. Brown, A. Khuri, and S. Krishnamurthy, *J. Am. Chem. Soc.*, **99**, 6237 (1977).
- (31) J. A. Gladysz and J. H. Merrifield, *Inorg. Chim. Acta*, **30**, L317 (1978).
- (32) R. Bau, S. W. Kirtley, T. N. Sorrell, and S. Winarko, *J. Am. Chem. Soc.*, **96**, 988 (1974).
- (33) P. J. Krusic, P. J. Fagan, and J. San Filippo, *J. Am. Chem. Soc.*, **99**, 250 (1977).
- (34) F. Basolo and R. G. Pearson, "Mechanisms of Inorganic Reactions", 2nd ed., Wiley, New York, 1967, pp 541, 553.
- (35) H. Alper, H. Des Abbayes, and D. Des Roches, *J. Organomet. Chem.*, **121**, C31 (1976).
- (36) C. J. Pickett and D. Pletcher, *J. Chem. Soc., Dalton Trans.*, 879 (1975).
- (37) J. A. Gladysz, J. L. Hornby, and J. E. Garbe, *J. Org. Chem.*, **43**, 1204 (1978).
- (38) J. A. Gladysz, V. K. Wong, and B. S. Jick, *J. Chem. Soc., Chem. Commun.*, 838 (1978); *J. Org. Chem.*, in press.
- (39) F. Calderazzo, *Inorg. Chem.*, **4**, 293 (1965).
- (40) J. K. Ruff and W. J. Schlientz, *Inorg. Synth.*, **15**, 84 (1974).
- (41) H. C. J. Ottenheijm and J. H. M. de Man, *Synthesis*, 163 (1975).
- (42) A. D. Beveridge and H. C. Clark, *J. Organomet. Chem.*, **11**, 601 (1968).
- (43) T. S. Piper and G. Wilkinson, *Naturwissenschaften*, **42**, 625 (1955).
- (44) H. R. H. Patil and W. A. G. Graham, *Inorg. Chem.*, **5**, 1401 (1966).
- (45) C. P. Casey, C. A. Bunnett, and J. C. Calabrese, *J. Am. Chem. Soc.*, **98**, 1166 (1976).
- (46) R. D. Gorsich, *J. Am. Chem. Soc.*, **84**, 2486 (1962).
- (47) R. A. Faltynek and M. S. Wrighton, *J. Am. Chem. Soc.*, **100**, 2701 (1978).
- (48) W. Malisch and M. Kuhn, *Chem. Ber.*, **107**, 979 (1974); A. D. Berry and A. G. MacDiarmid, *Inorg. Nucl. Chem. Lett.*, **5**, 601 (1969).
- (49) R. B. King and M. B. Bisnette, *J. Organomet. Chem.*, **2**, 15 (1964).
- (50) The synthesis of metal carbonyl monoanions by reaction of metal carbonyl dimers with KH has been recently reported: K. Inkrott, R. Goetze, and S. G. Shore, *J. Organomet. Chem.*, **154**, 337 (1978).

Contribution from the Institut de Recherches sur la Catalyse, 69626-Villeurbanne Cedex, France

Adduct Formation and Further Reactivity of Iron Carbonyl Complexes Introduced into a Zeolite Matrix

D. BALLIVET-TKATCHENKO* and G. COUDURIER

Received August 4, 1978

$\text{Fe}(\text{CO})_5$, $\text{Fe}_2(\text{CO})_9$, and $\text{Fe}_3(\text{CO})_{12}$ have been introduced into a dehydrated HY type zeolite. The iron content in the samples ranged from 1 to 4 wt %. During adsorption the iron complexes retain a molecular structure as shown by IR spectroscopy. For $\text{Fe}(\text{CO})_5$ and $\text{Fe}_2(\text{CO})_9$, a vacuum treatment leads to the evolution of CO and the formation of $\text{Fe}(\text{CO})_4$ bonded to the zeolite while in the case of $\text{Fe}_3(\text{CO})_{12}$ no CO is evolved. Treating $\text{Fe}_3(\text{CO})_{12}$ /zeolite under CO atmosphere restores the IR spectra of the $\text{Fe}(\text{CO})_5$ or $\text{Fe}_2(\text{CO})_9$ /zeolite system. Thereafter the zeolite acts both as an oxygen-containing ligand leading to L- $\text{Fe}(\text{CO})_4$ species and as a Lewis acid able to form adducts with $\text{Fe}_3(\text{CO})_{12}$ units via the oxygens of the bridging carbonyls. Heating the loaded zeolite (100–200 °C) produces a dehydroxylation of the support which is promoted by the iron carbonyls. The subsequent formation of CO_2 and hydrogen is explained by the water-gas shift reaction. Some CO_2 remains chemisorbed on the surface as evidenced by the presence of carbonate species. These species can be desorbed by hydrogen treatments with concomitant formation of CH_4 . Heating up to 250 °C leads to total decarbonylation of the iron carbonyl/HY systems and subsequent oxidation of Fe(0) to Fe(II) as evidenced by complexes formed with NO and CO. The oxidation process involves the protons of the zeolite. The Fe^{2+} ions are mainly located in the supercage in contrast to a conventional Fe^{2+}/Y sample.

Introduction

Coordination compounds supported on both organic and inorganic materials are attracting attention for the two main purposes of (i) anchoring coordination compounds in attempts to combine the advantages of homogeneous and heterogeneous catalysis^{1,2} and (ii) utilizing coordination complexes as precursors for the preparation of dispersed metallic catalysts.^{3,6}

The interaction between the support and the complex and the redox behavior of these partners are important factors which will influence the type of catalyst formed. With an

inorganic matrix, ions or metallic particles are obtained. Several types of inorganic matrices can be used, and among them the zeolites exhibit interesting properties associated with their unique structural features. The cavities, the inner electrostatic fields, and acidic and redox properties of the zeolites allow the introduction of transition-metal centers in sites of varying accessibilities.

Earlier work from this laboratory⁷ has shown that the adsorption of certain transition-metal carbonyls into an HY zeolite framework and subsequent thermal desorption leads

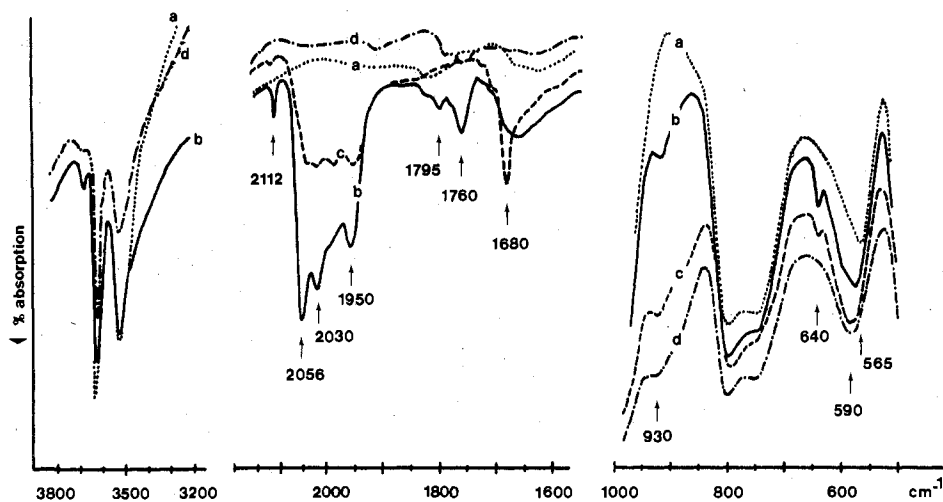


Figure 1. IR spectra of $\text{Fe}_3(\text{CO})_{12}/\text{HY}$ (1% Fe) decomposed under vacuum ($4000\text{--}400\text{ cm}^{-1}$): (a) spectrum of HY zeolite degassed at $350\text{ }^\circ\text{C}$, (b) spectrum after adsorption of $\text{Fe}_3(\text{CO})_{12}$ at $60\text{ }^\circ\text{C}$, (c) spectrum after decomposition at $100\text{ }^\circ\text{C}$, (d) spectrum after decomposition at $200\text{ }^\circ\text{C}$.

either to ions (Mo) or to metal (Re, Ru). This work has now been extended to binary carbonyl complexes of iron, i.e., $\text{Fe}(\text{CO})_5$, $\text{Fe}_2(\text{CO})_9$, and $\text{Fe}_3(\text{CO})_{12}$ since the resulting systems could be catalysts in the Fischer-Tropsch synthesis and other reductive transformations of CO. We wish to discuss here the behavior of $\text{Fe}(\text{CO})_5$, $\text{Fe}_2(\text{CO})_9$, and $\text{Fe}_3(\text{CO})_{12}$ in an HY zeolite framework as a function of temperature upon vacuum, CO, and H_2 treatments. The reaction was monitored by infrared and mass spectrometry and volumetric studies. Infrared spectroscopy was extensively used for providing information on a *molecular level* related to zeolite-adsorbate interactions and structural changes within the zeolite.

Experimental Section

Materials. The starting zeolite was a NaY faujasite supplied by Linde Co. (SK 40 sieves). A conventional exchange with NH_4Cl provides a NH_4Y zeolite (unit cell composition: $(\text{NH}_4)_{46}\text{Na}_{10}\text{Al}_{56}\text{Si}_{136}\text{O}_{384}$). Heating this sample for 15 h in oxygen and 3 h in vacuo (10^{-2} torr) at $350\text{ }^\circ\text{C}$ evolves NH_3 leading to the hydrogen form HY.

$\text{Fe}(\text{CO})_5$ and $\text{Fe}_2(\text{CO})_9$ were obtained from Ventron. $\text{Fe}_3(\text{CO})_{12}$ was prepared according to ref 8.

IR and Volumetric Experiments. IR spectra were recorded at $25\text{ }^\circ\text{C}$ on a Perkin-Elmer 125 spectrophotometer with a resolution of 4 cm^{-1} .

Compacting 5–8 mg of NH_4Y zeolite under 1 ton/cm^2 provided a wafer which was introduced into an IR cell equipped with KBr windows as previously described.⁹ A pretreatment as described above led to the obtention of the HY form. Then a break-seal device containing, under vacuum, the iron carbonyl complex was connected to the IR cell.

Adsorption of $\text{Fe}(\text{CO})_5$ takes place at room temperature while for $\text{Fe}_2(\text{CO})_9$ and $\text{Fe}_3(\text{CO})_{12}$ the HY wafer and the iron sample were warmed at $60\text{ }^\circ\text{C}$ in order to get a sufficient vapor pressure which allows rapid adsorption into the inorganic matrix. Then, at the same temperature, the IR cell is connected to a vacuum line (10^{-5} torr) so as to pump off the excess of iron carbonyl which has not been anchored. At this stage, the first IR spectra are recorded and are referred to as the initial spectra. Further thermal treatments are performed according to three procedures: (i) under vacuum, (ii) in a closed atmosphere after introduction of CO (300 torr) at $25\text{ }^\circ\text{C}$, (iii) in a closed atmosphere after introduction of H_2 (300 torr) at $25\text{ }^\circ\text{C}$.

The amount of iron carbonyl anchored is determined by chemical analysis. Most of the experiments deal with samples containing between 1 ± 0.2 and $4 \pm 0.2\%$ of iron. This corresponds to a loading of 3–12 Fe atoms per unit cell.

IR spectra of $\text{Fe}_3(\text{CO})_{12}$ and $\text{Fe}_2(\text{CO})_9$ were taken in KBr pellets and *n*-hexane solution and the spectrum of $\text{Fe}(\text{CO})_5$ was taken in a gas cell.

In the volumetric experiments, the introduction of the iron carbonyl was achieved as for the IR study. Gas evolution was monitored by a pressure gauge (Texas Instruments) and gaseous products were analyzed by mass spectrometry.

Iron analyses and mass spectra were performed at the Institut de Recherches sur la Catalyse.

Results

Adsorption of $\text{Fe}_3(\text{CO})_{12}$. Thermal Decomposition under Vacuum. Figure 1 reports the characteristic IR bands for after adsorption of $\text{Fe}_3(\text{CO})_{12}$ (followed by evacuation at the temperature of the adsorption) and then for increased thermal treatments under vacuum.

Adsorption of $\text{Fe}_3(\text{CO})_{12}$ on the HY zeolite is accompanied by a color change to green (visible adsorption λ_{max} 630 nm). No CO evolution is observed. In the ν_{OH} region, the 3640-cm^{-1} band decreases while a broad one develops near $3530\text{--}3520\text{ cm}^{-1}$. The CO stretching frequencies are centered at 2112 (mw), 2056 (s), 2030 (m), 1985 (sh), and 1950 cm^{-1} (m) for terminal carbonyls and at 1795 (mw) and 1760 cm^{-1} (m) for the bridging ones. In the low-frequency region ($1000\text{--}500\text{ cm}^{-1}$), new bands at 640 (mw) and 615 cm^{-1} (w) ($\delta_{\text{Fe-C-O}}$) and at 930 cm^{-1} (m) (zeolite framework) appear.

A progressive thermal decomposition under vacuum from 60 to $250\text{ }^\circ\text{C}$ changes the IR spectrum. The $3530\text{--}3520\text{-cm}^{-1}$ ν_{OH} broad band and the ν_{CO} and δ_{FeCO} bands disappear and the 3640- and 3540-cm^{-1} bands appear with a lower intensity. New bands develop at 1710 (w) and 1680 cm^{-1} (w) and at 1415 and 1370 cm^{-1} (vw); the two latter bands remain above $250\text{ }^\circ\text{C}$. This set of bands is not shifted by deuterium exchange. Positions of the bands due to the vibration of the zeolite framework are also modified. The band at 565 cm^{-1} shifts to 590 cm^{-1} , a shoulder near 700 cm^{-1} appears, and the 930-cm^{-1} band increases in intensity.

At the final temperature ($250\text{ }^\circ\text{C}$), the ν_{OH} 3640-cm^{-1} band is partially restored (for example, half of its initial intensity for the 12 Fe/unit cell sample) and approximately 12 mol of CO/mol of $\text{Fe}_3(\text{CO})_{12}$ have progressively appeared in the gas phase. It is important to note that at $200\text{ }^\circ\text{C}$ there is a simultaneous evolution of H_2 and CO_2 while at $250\text{ }^\circ\text{C}$ the formation of CH_4 is observed. The iron species are free of carbonyl ligands. The spectroscopic changes observed upon adsorption of molecular probes such as NO and CO are reported in Figure 2. The adsorption of CO (20 torr at $25\text{ }^\circ\text{C}$) leads to the appearance of a ν_{CO} band at 2193 cm^{-1} together with bands associated with gaseous and physically adsorbed CO. Evacuation of the sample at $25\text{ }^\circ\text{C}$ removes all the bands

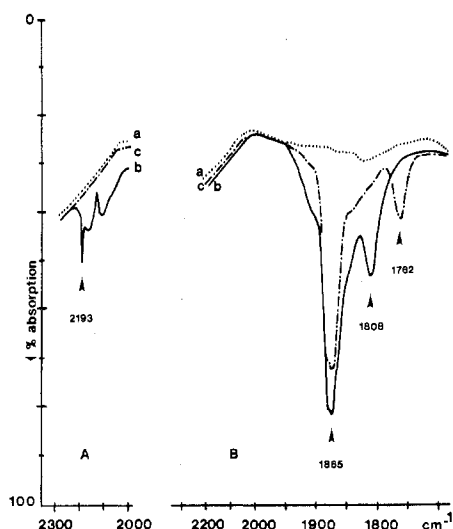


Figure 2. Total decarboxylation at 250 °C under vacuum of $\text{Fe}_3(\text{CO})_{12}/\text{HY}$ (1.2% Fe). IR spectra of adsorbed CO and NO (ν_{CO} and ν_{NO} region): (a) initial spectra, (b) spectra after (A) admission of 20 torr of CO at 25 °C and (B) admission of 20 torr of NO at 25 °C, (c) spectra after evacuation at 25 °C.

(Figure 2A). Upon NO exposure (20 torr at 25 °C), two intense bands are observed at 1865 and 1808 cm^{-1} with a shoulder at 1930 cm^{-1} . An evacuation at 25 °C for 1 h removes the band at 1808 cm^{-1} and decreases slightly the 1865 cm^{-1} one while a new species gives rise to an absorption centered at 1762 cm^{-1} (Figure 2B).

Adsorption of $\text{Fe}(\text{CO})_5$ and $\text{Fe}_2(\text{CO})_9$. Thermal Decomposition under Vacuum. Upon adsorption of $\text{Fe}(\text{CO})_5$ or of $\text{Fe}_2(\text{CO})_9$, the same spectra are obtained (ν_{CO} : 2112 (mw), 2040 (s), 2030 (sh), 2010 (s), 1985 (s), and 1950 cm^{-1} (ms)). Only those of $\text{Fe}(\text{CO})_5/\text{HY}$ are reported in Figure 3. The sublimation technique to load the zeolite with $\text{Fe}_2(\text{CO})_9$ produces some $\text{Fe}(\text{CO})_5$ in the gas phase. The dissociation reaction may partly explain the identical IR spectra obtained. This situation is not encountered during the loading with $\text{Fe}_3(\text{CO})_{12}$. In contrast to the spectrum recorded for $\text{Fe}_3(\text{CO})_{12}$, some $\nu_{\text{terminal CO}}$ bands are at lower frequencies and $\nu_{\text{bridging CO}}$ ones are absent even for $\text{Fe}_2(\text{CO})_9$. But similarly, the ν_{OH} bands are perturbed (decrease of the 3640 cm^{-1} one and appearance of the broad band at 3530–3520 cm^{-1}), and the additional band at 930 cm^{-1} (zeolite framework) appears. In the course of adsorption, a slight evolution of CO is observed, and after evacuation for 1 h at 60 °C, 1 ± 0.3 mol of

CO/mol of carbonyl complex ($\text{Fe}(\text{CO})_5$ or $\text{Fe}_2(\text{CO})_9$) is evolved whereas the color of the sample changes to green (visible absorption λ_{max} 630 nm). The IR spectra change with time to give finally that of the $\text{Fe}_3(\text{CO})_{12}$ sample (shift of the $\nu_{\text{terminal CO}}$ to higher frequencies, appearance of $\nu_{\text{bridging CO}}$ at 1795 and 1760 cm^{-1}). Then the thermal decomposition of these samples proceed as for the $\text{Fe}_3(\text{CO})_{12}$ -loaded one. After total decarbonylation, the same iron species are characterized by NO and CO adsorption.

During the decomposition of the $\text{Fe}(\text{CO})_5$ -loaded sample, the total volume of gas evolved has been checked. This corresponds to about 6.5 mol/mol of $\text{Fe}(\text{CO})_5$, i.e., 1 ± 0.3 mol of CO at 60 °C, 4 ± 0.3 mol of CO between 60 and 200 °C, and 1.5 ± 0.3 mol of H_2 between 120 and 200 °C. Trace amounts of CO_2 and CH_4 (<10% of H_2 evolved) are formed between 200 and 250 °C.

Thermal Decomposition of the Loaded Samples in Reducing Atmosphere. After metal carbonyl loading, a pressure of 300 torr of CO or H_2 was introduced into the IR cell at 25 °C, and the thermal decomposition was carried out.

Decomposition in CO Atmosphere. After admission at 25 °C, $\text{Fe}(\text{CO})_5$ - and $\text{Fe}_2(\text{CO})_9$ -loaded samples exhibit the same IR spectrum as that previously reported (Figure 3). In contrast, the IR spectrum of the $\text{Fe}_3(\text{CO})_{12}$ -zeolite system is modified and turns into that of these former samples with a red shift of the $\nu_{\text{terminal CO}}$ bands accompanied by the disappearance of the $\nu_{\text{bridging CO}}$ ones (Figure 4). The thermal decomposition proceeds in the same manner for the three samples. All the ν_{CO} bands are stable up to 180 °C and then suddenly disappear producing gaseous and physically adsorbed CO. The iron species formed do not adsorb CO but do adsorb NO as evidenced by the 1808- cm^{-1} band (1762 cm^{-1} after pumping off excess NO). The presence of bands at 3690 and 1605 cm^{-1} indicates the formation of water. A subsequent treatment in hydrogen atmosphere at 200 °C and evacuation at the same temperature regenerate the iron species already characterized by CO (ν_{CO} 2193 cm^{-1}) and NO (ν_{NO} 1930, 1865, and 1808 cm^{-1}) adsorptions.

Decomposition in H_2 Atmosphere. The decomposition of the three carbonyl-loaded samples proceeds roughly as under vacuum (Figure 5). The only difference is the presence of coordinated water (3690 and 1605 cm^{-1}) and adsorbed water (3500–1635 cm^{-1}) at temperatures higher than 150 °C which has to be related to the heat treatment in a closed cell. At 250 °C the iron species are free of carbonyl ligands. This typical decomposition procedure was repeated in the presence of 400 mg of $\text{Fe}_3(\text{CO})_{12}/\text{zeolite}$ introduced into the IR cell.

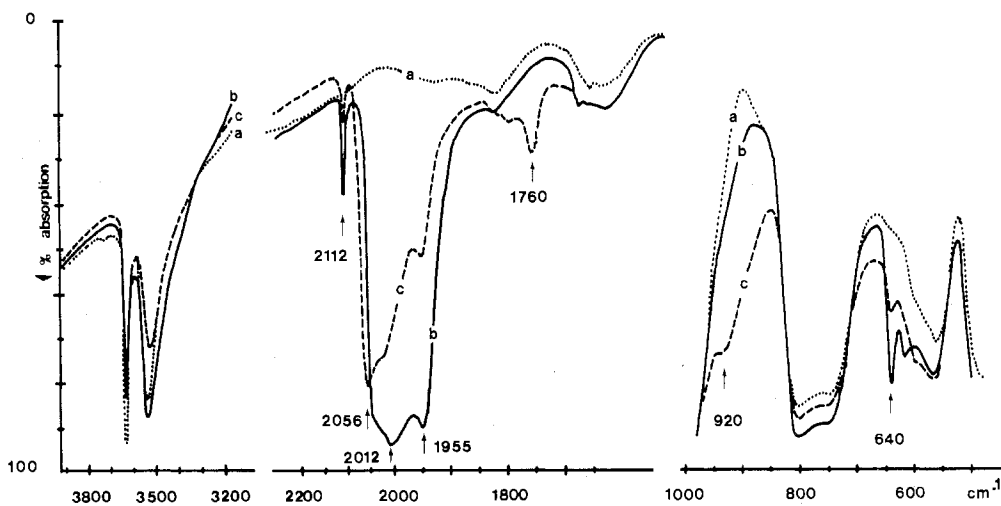


Figure 3. IR spectra of $\text{Fe}(\text{CO})_5/\text{HY}$ (1% Fe) decomposed under vacuum (400–400 cm^{-1}): (a) spectrum of HY zeolite degassed at 350 °C, (b) spectrum after adsorption of $\text{Fe}(\text{CO})_5$ at 25 °C, (c) spectrum after evacuation at 60 °C for 1 h.

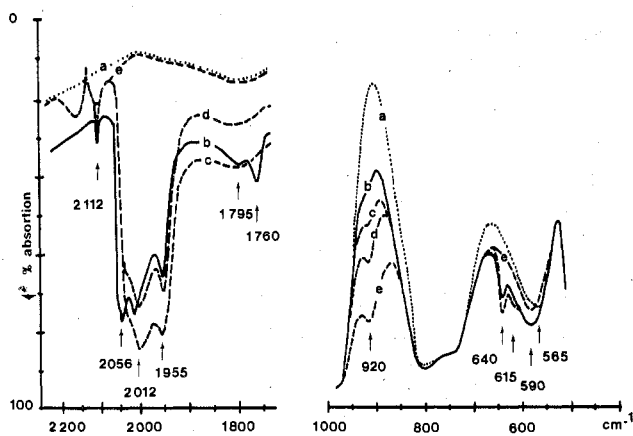


Figure 4. IR spectra of $\text{Fe}_3(\text{CO})_{12}/\text{HY}$ (0.8% Fe) decomposed under CO atmosphere (ν_{CO} and zeolite framework region): (a) spectrum of HY zeolite degassed at 350 °C, (b) spectrum after adsorption of $\text{Fe}_3(\text{CO})_{12}$ at 60 °C, (c) spectrum after admission of 300 torr of CO at 25 °C, (d) spectrum after heating at 120 °C for 1 h, (e) spectrum after heating at 200 °C for 1 h.

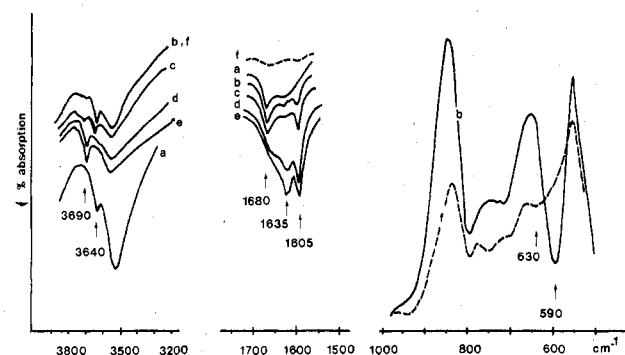


Figure 5. IR spectra of $\text{Fe}_3(\text{CO})_{12}/\text{HY}$ (0.8% Fe) decomposed under H_2 atmosphere (4000–400 cm^{-1}): (a) after adsorption of $\text{Fe}_3(\text{CO})_{12}$ at 60 °C, (b) after admission of 300 torr of H_2 and further heating at 100 °C, (c) after heating at 150 °C for 1 h, (d) after heating at 200 °C for 1 h, (e) after heating at 350 °C for 1 h, (f) after evacuation at 350 °C for 1 h.

As the temperature reaches 200 °C, CH_4 can be detected in the gas phase (ν_{CH} 3010 and $\delta_{\text{-CH}}$ 1303 cm^{-1}) as well as other saturated hydrocarbons (ν_{CH} 2950–2850 cm^{-1}). The iron species formed after total evolution of CO are unable to adsorb CO. NO admission results in the formation of ν_{NO} bands at 1915 (w), 1865 (w), and 1808 cm^{-1} (s). When the gas-phase NO is pumped off at 25 °C, the spectrum exhibits ν_{NO} bands at 1830 (m) and 1755 cm^{-1} (s) (Figure 6). Adsorption of CO (ν_{CO} at 2193 cm^{-1}) only occurs after evacuation of the samples at high temperature (200 °C) while the water bands disappear. At this step, NO admission restores the spectra of Figure 2B.

More drastic hydrogen treatments, i.e., 350 °C/16 h and 500 °C/16 h, lead to a decrease in ν_{OH} bands of the zeolite (3640 and 3540 cm^{-1}) with concomitant appearance of the water ones (3690 and 1605 cm^{-1}) and to the removal of bands at 1415–1370 cm^{-1} with concomitant appearance of CH_4 in the gas phase. Evacuation at 350 and 500 °C removes water and shifts the zeolite framework bands previously at 930 and 590 cm^{-1} , respectively, to 945 and 630 cm^{-1} (Figure 5). Readmission of H_2O restores the 3690–1605- cm^{-1} absorptions and shifts the 630 one to 590 cm^{-1} and the 945 one to 930 cm^{-1} , this phenomenon being reversible. The reactivity toward oxygen (150 torr) was also checked at increasing temperatures on an H_2 -treated sample evacuated at 350 °C. During the warm-up program, the 630- and 945- cm^{-1} bands are respectively shifted to 565 and 890 cm^{-1} (Figure 7). Water adsorption induces no significant modifications on the 890- cm^{-1}

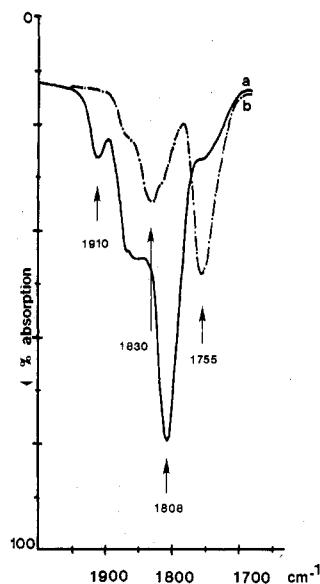


Figure 6. IR spectra of the sample depicted in Figure 5e (ν_{NO} region): (a) after admission of 20 torr of NO, (b) after evacuation at 25 °C.

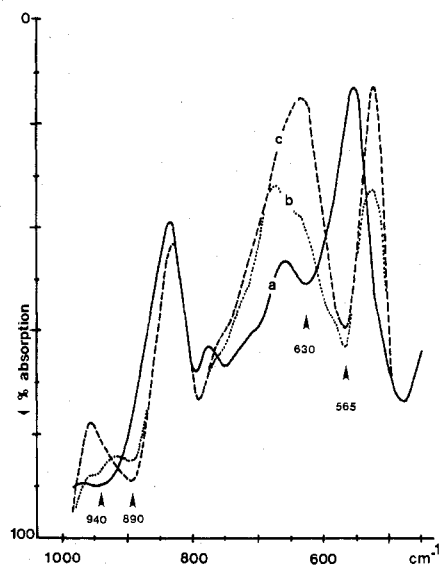


Figure 7. IR spectra of $\text{Fe}(\text{CO})_5/\text{HY}$ (4.3% Fe) evacuated at 250 °C with further treatments under hydrogen and oxygen (zeolite framework region): (a) H_2 treatment at 350 °C and evacuation at 350 °C, (b) admission of 300 torr of O_2 at 350 °C for 1 h, (c) admission of 300 torr of O_2 at 350 °C for 16 h.

band, whereas H_2 treatment at 350 °C followed by evacuation restores the initial spectrum. The foregoing data indicate that the dehydration, hydration, oxidation and reduction reactions are reversible processes.

Discussion

The HY form has three types of hydroxyl groups (3740 (w), 3640 (s), and 3540 cm^{-1} (s)). The 3740- cm^{-1} band has been attributed to hydroxyls terminating the crystal lattice. In most cases these groups are inert. The 3640- and 3540- cm^{-1} bands are attributed to $-\text{OH}$ groups respectively located in the supercage ($-\text{O}_1\text{H}$) and in the hexagonal prisms ($-\text{O}_3\text{H}$).^{10,11}

Vibrations of the zeolite framework have been extensively studied by Flanigen.¹² They occur in the 1200–400- cm^{-1} region for the internal vibrations of the SiO_4 and AlO_4 tetrahedra and for the vibrations of the linkages between tetrahedra. The vibrations are not specifically assigned to SiO_4 or AlO_4 groups but to the vibrations of $(\text{Si,Al})\text{O}_4$ groups designed as TO_4 . They are related to the Si,Al composition

Table I. Carbonyl Stretching Frequencies for Iron Carbonyl Compounds and Adducts with AlBr₃ and HY

carbonyl compd	$\nu_{\text{CO}}(-\text{CO})$, cm ⁻¹	$\nu_{\text{CO}}(>\text{CO})$, cm ⁻¹
Fe ₃ (CO) ₁₂ ^a	2058 s, 2053 s, 2036 s	1871-1862 w, 1823 m, br
Fe ₃ (CO) ₁₂ ^b	2097 w, 2056 s, sh, 2039 s, 2018 s, sh, 2006 sh, 1987 sh	1855 w, 1825 mw
Fe ₃ (CO) ₁₂ ^c	2103 w, 2046 vs, 2023 mb, 2013 sh	1867 w, 1838 mw
Fe ₃ (CO) ₁₂ /AlBr ₃ ^d	2124 w, 2081 ms, 2070-2008 s, b	1922 mw, 1548 s
Fe ₃ (CO) ₁₂ /HY	2112 mw, 2056 s, 2030 m, 1985 sh, 1950 m	1795 mw, 1760 m
Fe(CO) ₅ ^e	2030 ms, 2010 s	
LFe(CO) ₄ ^f	2040 m, 1970 m, 1940 vs	
Fe(CO) ₅ /HY	2112 mw, 2040 s, 2030 sh, 2010 s, 1985 sh, 1950 ms	

^a In argon matrix; ref 14. ^b In KBr pellets; this work. ^c *n*-Hexane solution; this work. ^d Reference 16. ^e Gas phase, 0.5 torr; this work. ^f Reference 17.

and to the T-O bond order. In the HY zeolite, the asymmetric and symmetric stretching vibrations of TO₄ units are respectively observed at ~1200 (sh) and ~1000 cm⁻¹ (vs) (internal and external modes) and at 795 (ms) and 745 cm⁻¹ (ms) (internal and external modes). The TO₄ deformations are observed at 460 cm⁻¹ (s) and those of the rings of six TO₄ units constituting the faces of the hexagonal prisms at 565 cm⁻¹ (m) (band of the R-6 ring). The IR changes of the Y form exchanged with transition-metal cations have been correlated with the location of these ions.^{12,13}

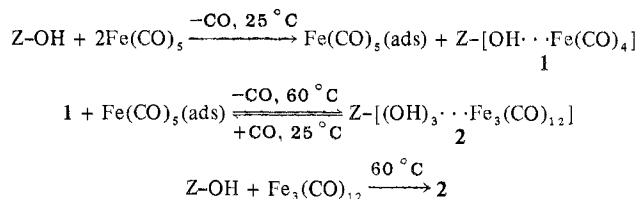
Nature of the Interaction of Carbonyl Complexes with Zeolite upon Adsorption and Decomposition. The size of the mono-, di-, and trinuclear iron carbonyl complexes allows them to enter only in the supercage of the zeolite.

At the initial step, the Fe₃(CO)₁₂/HY system does not evolve carbon monoxide, and the IR spectrum exhibits absorptions in the ν_{CO} region of the bridging ligand. These experimental observations show that the Fe₃(CO)₁₂ complex is linked to the zeolite. The way of anchoring is determined by the comparison of ν_{CO} for different Fe₃(CO)₁₂ samples (Table I). The Fe₃(CO)₁₂/HY system exhibits an IR spectrum which tends to approximate the structure of Fe₃(CO)₁₂ in solution for which a threefold axis of symmetry is proposed.¹⁵ Nevertheless, high-frequency shifts for the ν_{CO} of terminal ligands (10 cm⁻¹) and low-frequency shifts for the ν_{CO} of bridging ligands (80 cm⁻¹) are in agreement within the values reported by Shriver et al.^{16a-c} for the adduct Fe₃(CO)₁₂·AlBr₃. However in our case, since all the bridging CO's are affected with weaker frequency shifts and the -O₁H hydroxyl groups are perturbed, the interaction must be through all the bridging CO's with a weaker Lewis acid, the protons of the HY zeolite being located in the supercage.¹¹ Very recently Shriver et al.^{16d} have described the first example of a carbonyl cluster, H₂Fe₃(CO)₁₁, in which a proton is bonded to the oxygen of a bridging carbonyl ligand. This complex prepared in solution is stable only at low temperature, and no IR data have been reported.

As the Fe₃(CO)₁₂ unit tends to acquire a C_{3v} symmetry, it may be assumed that the iron complex is located near the supercage windows along the threefold symmetry axis of the zeolite as already observed in the case of Mo(CO)₆.⁷ This assumption is corroborated by the induced modifications in the IR spectrum of the zeolite framework. Asymmetric and symmetric stretching vibrations of some TO₄ units are respectively shifted to 930 and 700 cm⁻¹ while the R6 vibration band (hexagonal prisms) is not affected.

Adsorptions of Fe(CO)₅ and Fe₂(CO)₉ on the HY zeolite provide IR spectra which are assigned to that of Fe(CO)₅(ads) superimposed with that of a monosubstituted species, such as L-Fe(CO)₄¹⁷ (Table I). The zeolite, by the presence of its hydroxyl groups, is capable of stabilizing the unsaturated species Fe(CO)₄ (1, Scheme I). Thus, the surface reaction proceeds via the substitution of one carbonyl ligand by one lattice oxygen. A subsequent heating of the sample under vacuum up to 60 °C initiates the migration of the Fe(CO)₄ moieties and then aggregation to finally form the same adduct

Scheme I



(2, Scheme I) as is obtained directly from Fe₃(CO)₁₂. At this point exposure to carbon monoxide reverses these steps. Scheme I depicts the reactions where Z denotes the zeolite framework. The chemistry in solution^{17,18} or in low-temperature matrices¹⁹ of the same iron carbonyl complexes also involves substitution and aggregation reactions in which Fe(CO)₄ has often been postulated as the intermediate. In this work Fe(CO)₄ can be characterized thanks to the zeolite matrix which acts as a rigid ligand and stabilizes the unsaturated coordination compound. Alumina has already been described to exhibit such properties vs. only two kinds of coordination compounds, i.e., Mo(CO)₆²⁰ and rhodium carbonyl clusters.²¹

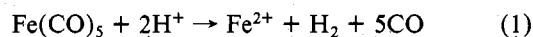
During the thermal treatment under vacuum, gradual decarbonylation occurs. Discrete intermediates cannot be identified with any confidence. The decarbonylation process is complete after outgassing at 200 °C and is accompanied on one hand by the migration of some iron species toward more inaccessible sites (sodalite cavity and hexagonal prism) as shown by changes in the vibration region of the zeolite framework and on the other hand by H₂, H₂O, CO₂, CH₄ and saturated hydrocarbons formations. The set of hydrogen-containing products is not observed when the zeolite does not exhibit hydroxyl groups (NaY commercial sample treated under vacuum at 350 °C). Water formation is due to a dehydroxylation of the zeolite which starts at low temperature (ca. 120 °C). This process has to be associated with the presence of iron carbonyl species since the zeolite pretreated at 350 °C prior to the adsorption of the carbonyl complexes contains no more water molecules but only OH groups as shown by IR spectra. In the same temperature range (ca. 120 °C), hydrogen formation also begins to occur. Since hydrogen formation implies a redox reaction, the other partners can be CO and/or the iron moiety. Experimentally, CO₂ is detected in the gas phase at 200 °C while the 1415- and 1370-cm⁻¹ bands appearing at lower temperature may be attributed to carbonate species resulting from the chemisorption of CO₂ on the zeolite.²² It is noteworthy that a hydrogen treatment removes the 1415- and 1370-cm⁻¹ bands and leads to CH₄ formation. In our opinion, the presence of H₂ and CO₂ is relevant for the water-gas shift reaction which is promoted by iron carbonyl complexes.²³ Further experiments performed on a Fe₃(CO)₁₂/NaY sample under the water-gas shift conditions, at 120 °C, corroborate this assumption. However, the discrepancy between the mass balance of H₂ and CO₂ observed in the case of Fe₃(CO)₁₂/HY points out that other redox reactions are involved as explained below.

Iron Species Obtained by Total Evolution of CO. Little information is available in the literature concerning the iron/zeolite systems.^{4,24,25-27} However, Lunsford et al.²⁴ have studied several Fe²⁺-exchanged Y zeolites. In particular their results concerning NO adsorption and modification of the IR spectra induced by vacuum treatment are comparable to ours. Two ν_{NO} bands at 1890 and 1778 cm⁻¹ have been associated, respectively, with a high-spin state ($S = 3/2$) and a low-spin state ($S = 1/2$) mononitrosyl iron complex. In these complexes, the other ligands are the lattice oxygens, and both complexes seem to be located in the supercage. In our work the ν_{NO} bands are centered at 1865 and 1762 cm⁻¹. The same evolution is observed upon vacuum treatment. However, the small deviations observed for ν_{NO} compared to those of ref 23 may be associated to differences in the origins of the respective samples. No bands due to N₂O (2200 cm⁻¹) or iron oxide (ν_{FeO} 600 cm⁻¹) have been detected. Consequently Fe(0) is oxidized into Fe(II) species which are able to form coordination complexes with NO. The zeolite framework acts as a rigid ligand leading to unusual geometries which induce different spin states. The same situation has been recently described in solution with potentially tetradentate ligands.²⁸ According to Enemark and Feltham's notation,²⁹ we deal with a Fe(NO)⁷ electron configuration. This particular configuration has already been identified in coordination chemistry by means of X-ray, Mössbauer, EPR, and IR techniques. The ligand systems encountered consist essentially of polydentate ones such as tetraphenylporphyrin dianions,³⁰ *o*-phenylenebis(dimethylarsine)³¹ sulfur-containing ones,³² and monodentate ones such as CN⁻³³ and H₂O.³⁴ The ν_{NO} fall within the range 1845–1620 cm⁻¹ which are associated with both "linear" and "bent" NO ligands. The Fe(II)/zeolite/NO systems thus afford a new example of (FeNO)⁷ complexes where the oxygens of the zeolite act as polydentate ligands. The ν_{NO} observed agree well with the values reported above. But in the absence of X-ray data, the geometry of the complexes has yet to be confirmed.

It should be pointed out that in our experiments iron metallic particles could be formed as well as Fe²⁺ ions. It has been shown that the adsorption of nitric oxide on metallic iron is accompanied by two intense bands at 1810–1800 (s) and 1720 cm⁻¹ (m).³⁵ The high-frequency band has been attributed to NO adsorbed on oxidized iron (ν_{FeO} 600 cm⁻¹) and the low-frequency one to NO adsorbed on metallic Fe particles. Our results are quite different and show that the majority of the iron is in the 2+ state. Adsorption of carbon monoxide also occurs on metallic iron^{36,37} and on a variety of cations such as Fe²⁺ located in a zeolite framework.²⁷ With silica-supported metallic iron,³⁶ ν_{CO} bands are centered at 2020, 1980, and 1887 cm⁻¹ and are stable up to 180 °C. On the other hand, CO adsorbed on Fe(II)/HY samples exhibits only one band at 2198 cm⁻¹ which disappears either on pumping at 25 °C or by the introduction of small amounts of water.²⁷ Our results fit well with the latter one thereby arguing against the presence of iron particles. The appearance of a ν_{CO} frequency higher than that of gaseous CO (2153 cm⁻¹) is rather striking. It is a general phenomenon when CO is adsorbed on cations present in an inorganic matrix,²⁷ but it has been rarely encountered in the case of coordination complexes.³⁸ Explanation based on pure σ bonding between CO and the ion has been proposed; however a new mode of coordination (i.e., isocarbonyl behavior) could be involved.

Another iron oxidation state may also be present, i.e., Fe³⁺. This hypothesis arises from the observation that 1.5 ± 0.3 mol of H₂ is evolved/g-atom of iron during the decomposition of the carbonyl complex. However it does not appear to us as a relevant proposal for the following reasons. Fe³⁺- and Fe²⁺-exchanged Y zeolites (exchange level 65%) have been

prepared. The Fe³⁺/Y sample does not adsorb CO and exhibits the 875-cm⁻¹ band. A reductive treatment under H₂ at 200 °C produces water, and further evacuation permits CO adsorption (ν_{CO} 2193 cm⁻¹). Moreover, the 875-cm⁻¹ band is shifted toward 930 cm⁻¹. According to the literature,²⁶ Fe³⁺ has been reduced to Fe²⁺. Starting with Fe²⁺/Y sample, CO adsorption occurs (ν_{CO} 2193 cm⁻¹), and the 930-cm⁻¹ band is present. An oxygen treatment restores the characteristics of an Fe³⁺/Y sample.²⁶ As the behavior of a genuine Fe²⁺/Y sample fits quite well with that of the decarbonylated iron carbonyl/HY system, Fe³⁺ ions are not the predominant species in the last system. Moreover, iron carbonyl complexes such as Fe(CO)₅ are oxidized in acidic solution³⁹ according to reaction 1.



Mobility of the Iron Species. Carbon monoxide and nitric oxide adsorption provide additional information on the location of the Fe²⁺ ions since CO enters only the supercage of the zeolite framework whereas NO enters both the supercage and the sodalite.¹¹ It follows that most of the Fe(II) must be located in the supercage (sites II and II'). Their migration toward the hexagonal prism and the sodalite cavity takes place upon vacuum treatment from 200 to 350 °C. This particular cation distribution is observed in the case of Fe²⁺-exchanged Y zeolite.¹³

The low-spin complex (FeNO)⁷ is only formed when decomposition of the iron carbonyls occurs in CO atmosphere. Decomposition in a H₂ atmosphere (Figure 6) causes the formation of several species. The low-spin (ν_{NO} 1755 cm⁻¹) and the high-spin (ν_{NO} 1865 cm⁻¹) complexes are present together with another species characterized by ν_{NO} 1830 cm⁻¹. In respect to Figure 2B the relative concentration of each species is reversed. Reversible CO adsorption occurs if the water has been pumped off at elevated temperatures. This can be accounted for by the stronger coordination properties of H₂O than CO to Fe(II).

As already observed,⁴⁰ hydrogen treatment at 350 or 500 °C does not lead to iron particles but induces the migration of Fe(II) toward the hexagonal prism (R6 band at 630 cm⁻¹). At this stage, oxidation by molecular oxygen at increasing temperatures produces a migration of the iron toward site SI' in order to form Fe–O–Fe bridges which is in accord with the results of Boudart et al.¹³ If the relocation of Fe³⁺ ions in more accessible sites is well proven, we think that the band at 890 cm⁻¹ corresponds to a red shift of the 930-cm⁻¹ band and should be assigned to a $\nu_{\text{as}} \text{TO}_4$ vibration (bond order weakened by the oxidation of Fe²⁺ to Fe³⁺). This assumption is strengthened by our experiments on Fe³⁺- and Fe²⁺-exchanged Y zeolite where this band is only observed in the case of Fe³⁺/Y samples.

Conclusion

The present study has revealed that a zeolite cannot only act as a multifunctional polydentate ligand (ligand substitution reaction and adduct formation) but also as a protic acid promoting redox reaction and the conversion of coordinated CO into hydrocarbons.

Fe(CO)₅, Fe₂(CO)₉, and Fe₃(CO)₁₂ can all be introduced into a zeolite framework while retaining a molecular structure. Starting with Fe(CO)₅ or Fe₂(CO)₉, the initial adduct undergoes a substitution of one CO by one oxygen lattice to give a mononuclear iron carbonyl-zeolite complex. Subsequently the iron carbonyl species migrate to form polynuclear iron carbonyl complexes which are retained in the zeolite cavities via a Lewis acid-bridging carbonyl interaction. Heating these samples induces decarbonylation and favors redox reaction with the zeolite thus promoting the oxidation of iron to the 2+ state (the maximum exchanged level corresponds to 9%

in iron loading). The foregoing reactions are accompanied by the formation of 1.5 mol of H₂/g-atom of iron and trace amounts of CO₂ and saturated hydrocarbons. Therefore, several reactions occur in parallel, and the different elementary steps are presently under study, especially in correlation with the reactivity of carbon oxides (CO and CO₂) toward water and hydrogen. This work has shown that chemisorbed CO₂ reacts with H₂ to produce CH₄, and CO reacts with H₂O to produce the water-gas shift reaction.

The Fe(II) species have been characterized by complex formation with NO ((FeNO)⁷ electron configuration) and CO. Decomposition at mild temperatures leads to location of the ions mainly in accessible sites (supercage, sodalite cavity) whereas a more drastic treatment induces their migration into the inaccessible sites (hexagonal prism). The present method is clearly superior to the conventional exchange ones for the introduction of Fe²⁺ ions into the molecular sieve pores. The advantages of this method are that it does not damage the crystalline structure, permits the location of the ions in more accessible sites, and does not introduce counteranions which can be trapped as impurities during the exchange process.

Acknowledgment. We thank Drs. R. P. A. Sneed and I. Tkatchenko for stimulating discussions. We gratefully acknowledge support of this research by CNRS (ATP Epargne d'énergie et Opérations chimiques industrielles).

Registry No. Fe(CO)₅, 13463-40-6; Fe₂(CO)₉, 15321-51-4; Fe₃(CO)₁₂, 17685-52-8.

References and Notes

- (1) See for example, "Proceedings of the 2nd International Symposium on the Relations between Homogeneous and Heterogeneous Catalytic Phenomena", *J. Mol. Catal.*, **3** (1977), and references therein.
- (2) J. Robertson and G. Webb, *Proc. R. Soc. London, Ser. A*, **341**, 383 (1974).
- (3) J. R. Anderson, P. S. Elmes, R. F. Howe, and D. E. Mainwaring, *J. Catal.*, **50**, 508 (1977).
- (4) C. R. Castor and R. M. Milton, U.S. Patent 3 013 987 (1958); *Chem. Abstr.*, **61**, 3969a (1964).
- (5) E. G. Derouane, J. B. Nagy, and J. C. Vedrine, *J. Catal.*, **46**, 434 (1977).
- (6) P. Gelin, Y. Ben Taarit, and C. Naccache, *J. Catal.*, submitted for publication.
- (7) P. Gallezot, G. Coudurier, M. Primet, and B. Imelik, *ACS Symp. Ser.*, **No. 40**, 144 (1977).
- (8) W. McFarlan and G. Wilkinson, *Inorg. Synth.*, **8**, 181 (1966).
- (9) M. V. Mathieu and P. Pichat, "Catalyse au laboratoire et dans l'industrie", B. Claudel, Ed., Masson, Paris, 1967, p 319.
- (10) D. M. Olson and E. Dempsey, *J. Catal.*, **18**, 154 (1970).
- (11) J. W. Ward, *ACS Monogr.*, **No. 171**, 118 (1976).
- (12) E. Flanigen, *ACS Monogr.*, **No. 171**, 80 (1976).
- (13) R. A. Dalla Betta, R. L. Garten, and M. Boudart, *J. Catal.*, **41**, 40 (1976).
- (14) M. Poliakoff and J. J. Turner, *J. Chem. Soc., Chem. Commun.*, 1008 (1970).
- (15) D. B. W. Yawney and F. G. A. Stone, *J. Chem. Soc. A.*, 502 (1969); J. Knight and M. J. Mays, *J. Chem. Soc., Chem. Commun.*, 1006 (1970).
- (16) (a) A. Alich, N. J. Nelson, D. Stroppe, and D. F. Shriver, *Inorg. Chem.*, **11**, 2976 (1972); (b) N. E. Kim, N. J. Nelson, and D. F. Shriver, *Inorg. Chim. Acta*, **7**, 393 (1973); (c) J. S. Kristoff and D. F. Shriver, *Inorg. Chem.*, **13**, 499 (1974); (d) H. A. Hodali, D. F. Shriver, and C. A. Ammlung, *J. Am. Chem. Soc.*, **100**, 5239 (1978).
- (17) M. Bigorgne, *J. Organomet. Chem.*, **24**, 211 (1970); P. Cataliotti, A. Foffani, and L. Marchetti, *Inorg. Chem.*, **10**, 1594 (1971).
- (18) K. Noack and M. Ruch, *J. Organomet. Chem.*, **17**, 309 (1969); I. Fischler, K. Hildenbrand, and E. Koerner von Gustorf, *Angew. Chem.*, **87**, 3517 (1975).
- (19) M. Poliakoff and J. J. Turner, *J. Chem. Soc., Dalton Trans.*, 2276 (1974).
- (20) A. Brenner and R. L. Burwell, Jr., *J. Am. Chem. Soc.*, **97**, 2565 (1975); *J. Catal.*, **52**, 353 (1978).
- (21) G. C. Smith, T. P. Chojnacki, S. R. Dasgupta, J. Iwatate, and K. L. Watters, *Inorg. Chem.*, **14**, 1419 (1975).
- (22) P. A. Jacobs, F. H. Van Cauwelaert, E. F. Vansant, and J. B. Uytterhoeven, *J. Chem. Soc., Faraday Trans. 1*, **69**, 1056 (1973).
- (23) H. C. Kang, C. H. Mauldin, T. Cole, W. Slegeir, K. Cann, and R. Pettit, *J. Am. Chem. Soc.*, **99**, 8323 (1977).
- (24) J. W. Jermyn, T. J. Johnson, E. F. Vansant, and J. H. Lunsford, *J. Phys. Chem.*, **77**, 2964 (1973).
- (25) D. W. Collins and L. N. Mulay, *IEEE Trans. Magn.*, **4**, 470 (1968).
- (26) W. N. Delgass, R. L. Garten, and M. Boudart, *J. Phys. Chem.*, **73**, 2970 (1969); R. L. Garten, W. N. Delgass, and M. Boudard, *J. Catal.*, **18**, 90 (1970).
- (27) C. L. Angell and P. C. Schaffer, *J. Phys. Chem.*, **70**, 1413 (1966).
- (28) L. Sacconi, C. A. Ghilardi, C. Healli, and F. Zanobini, *Inorg. Chem.*, **14**, 1380 (1975).
- (29) J. H. Enemark and R. D. Feltham, *Coord. Chem. Rev.*, **13**, 339 (1974).
- (30) W. R. Scheidt and M. E. Frisse, *J. Am. Chem. Soc.*, **97**, 17 (1975); W. R. Scheidt and L. M. Piciulo, *ibid.*, **98**, 1913 (1976); B. B. Wayland and L. W. Olson, *ibid.*, **96**, 6037 (1974).
- (31) J. H. Enemark, R. D. Feltham, B. T. Huie, P. L. Johnson, and J. Bizot-Swedo, *J. Am. Chem. Soc.*, **99**, 3285 (1977).
- (32) B. A. Goodman, J. B. Raynor, and M. C. R. Symons, *J. Chem. Soc. A*, 2572 (1969); M. P. Halton, *Inorg. Chim. Acta*, **8**, 137 (1974).
- (33) R. Nast and J. Schmidt, *Angew. Chem., Int. Ed. Engl.*, **8**, 383 (1969); J. Schmidt, H. Kuhr, W. D. Dorn, and J. Kopf, *Inorg. Nucl. Chem. Lett.*, **10**, 55 (1974).
- (34) W. P. Griffith, J. Lewis, and G. Wilkinson, *J. Chem. Soc.*, 3993 (1958).
- (35) G. Blyholder and M. C. Allen, *J. Phys. Chem.*, **69**, 3998 (1965); H. Bandow, T. Onishi, and K. Tamaru, *Chem. Lett.*, 83 (1978).
- (36) G. Blyholder and L. D. Neff, *J. Phys. Chem.*, **66**, 1464 (1968).
- (37) R. P. Eischens and W. A. Pliskin, *Adv. Catal.*, **10**, 1 (1958); G. D. Blyholder, *J. Chem. Phys.*, **36**, 2036 (1962).
- (38) R. J. Irving and E. A. Magnussen, *J. Chem. Soc.*, 1860 (1956); *ibid.*, 2283 (1958); C. W. de Kock and D. A. Leirsburg, *J. Am. Chem. Soc.*, **94**, 3235 (1972).
- (39) J. Dewar and H. O. Jones, *Proc. R. Soc. London, Ser. A*, **71**, 427 (1903).
- (40) Y. Y. Huang and J. R. Anderson, *J. Catal.*, **40**, 143 (1975).

Contribution from the Institut für Anorganische Chemie der Universität Köln, D-5 Köln 41, West Germany, and Fraunhofer Gesellschaft, Institut für Treib- und Explosivstoffe, D-7507 Pfinztal-Berghausen, West Germany

The Oxidation Product of (β -Phthalocyaninato)chromium(II)

K. H. NILL, F. WASGESTIAN,* and A. PFEIL

Received April 27, 1978

The oxidation of (β -phthalocyaninato)chromium(II) by molecular oxygen gives a product with a 1:1 ratio of chromium to oxygen atoms. From infrared and Raman spectra, magnetic data, and mass spectra of the product, obtained by reaction of (β -phthalocyaninato)chromium(II) with ¹⁸O₂, ¹⁶O¹⁸O, and ¹⁸O₂, it was characterized as an oxo(phthalocyaninato)chromium(IV) dimer.

Introduction

Elvidge and Lever¹ reported that Cr^{III}PcOH (Pc denotes the phthalocyanine moiety) is formed as long purple needles on repeated sublimation of a mixture of Cr^{II}Pc and Cr^{III}PcOH, which was obtained by reacting phthalodinitrile with chromium(III) acetate.

*To whom correspondence should be addressed at the Institut für Anorganische Chemie der Universität Köln.

By this method Ercolani² also obtained a purple-red crystalline compound, which he denoted product I. His compound, however, was sensitive to air which is usually not observed for a phthalocyanine containing chromium in the oxidation state III. On exposure to air, product I changed into a blue-violet product (II) with properties different from those described by Elvidge and Lever¹ for Cr^{III}PcOH. Product I could be repeatedly sublimed but remained sensitive to air. It did not contain oxygen. By its composition, magnetic